DETERMINATION OF AQUIFER PARAMATERS USING GENERATED WATER LEVEL DISTURBANCES

A. M. Wasantha Lal [1]

A method was developed to determine bulk values of aquifer and sediment parameters in a coupled canal-aquifer system using generated sinusoidal water level disturbance. The method is based on analytical solutions to canal-aquifer interaction derived in terms of dimensionless parameters. Numerical models were used to verify the behavior of the solutions in selected test problems. The method was applied to determine physical parameters of the L-31W canal in Miami-Dade County, Florida near the Everglades explicitly both in dimensionless and dimensional forms. The physical parameters were derived using data collected from a field experiment that was carried out using operational control features of the regional water management system.

Results of the analysis show that various dimensionless parameter groups determine dynamic behaviors of both confined and unconfined aquifers during canal-aquifer interaction. Which seepage process dominates in the system depends on the range of a particular dimensionless parameter. The analytical relationships developed in the paper are useful for calculating parameters in large regional systems where the historical data are noisy or questionable. These relationships make it possible to use measured stresses applied to the system in order to create recognizable signatures that can be used with relationships between the input and output signals to determine the parameters. Sinusoidal stresses were used in the current test, and the resulting parameter values are expressed in both dimensionless and dimensional forms.

[1]Lead Engineer and Supervising Engineer, Model Development Division, South Florida Water Management District, 3301 Gun Club Rd., West Palm Beach, FL 33406

INTRODUCTION

Quantification and control of groundwater flow and canal seepage in South Florida have become important concerns because of the role they play in management of the hydrology. Water management involves resolving problems created by competing and conflicting needs to access or control water. In this region, too much water is present during wet periods which must be routed away to tides or storage areas to be used during dry periods. During dry periods water is needed to meet demands in the agricultural and urban areas, satisfy environmental needs, control salinity in coastal areas, and restore natural areas such as the Everglades. Management of natural wetlands that are located next to urban and agricultural areas is an extremely difficult task considering that the water levels maintained for various land use types are different and the underlying limestone-based aquifer is extremely porous. The hydrologic system in southern Florida is complex due to the presense of canals that allow for the conveyance of water in and out of Lake Okeechobee, dikes and levees that create regional impoundments (water conservation areas), urban areas and natural areas. Any future restoration of natural areas could be accomplished only by ensuring that water supply and flood control needs in the urban and agricultural areas are not affected. In order to achieve all these goals, a good understanding of surface water flow, groundwater flow, and stream-aquifer interaction in canals is needed along with accurate estimates of underlying physical parameters. In the specific case of study site L-31W shown in Figure 1, determination of groundwater flow and canal seepage parameters is important in necessary in order to understand and control groundwater flow and canal seepage out of the Everglades National Park (ENP), minimize impacts of urban well fields, and manage freshwater base flow to Biscayne Bay. This manuscript describes a field test that can be used to determine aquifer parameters, and an analytical solution that can be used to calibrate aquifer and canal seepage parameters.

In South Florida, calibration of regional parameters is not a simple process because the physical system itself is not simple and the state variables of the system depend heavily on complicated operational rules. A typical water level or discharge time series in South Florida shows primarily the effects of rainfall and evapotranspiration (ET) stresses over with the effects of local and regional stresses due to structure and pump operations by public water supply users, industrial

users and agricultural users superimposed. Under these conditions, a calibration based on optimization or manual methods also has a limited use, partly because of the noise generated during the operations. Some of the calibration methods fail when the level noise in the historical data due to unmeasured natural and operational stresses are extremely high. One reason for the difficulty of calibrating such a system is the lack of understanding of the cause and effect relationships of hydrologic stresses and hydrologic responses.

The problem of parameter estimation of integrated models is complicated for other reasons as well. Since many integrated models are under-determined, it is difficult to obtain high parameter resolutions and low parameter errors when the data is noisy and the data collection network is sparse (Lal, 1998). Many of the numerical models for integrated systems are under determined because of the overuse of physical parameters. Even when the values of some of the parameter groups can be determined, resolution of the individual physical parameters can be difficult at times. In the case of the calibration of groundwater flow for example, hydraulic head data can be used to determine aquifer diffusivity, but not individual parameters for transmissivity and storativity. A second condition such as a steady state or a known discharge, is required to solve this problem. The result of using poorly calibrated or resolved parameters is large output uncertainty. When this happens, use of a model is limited to the locations where good data is available for the calibration.

Field testing is often used in the past on a number of occasions to determine aquifer parameters. Many of the field testing methods make use of analytical or numerical models. A comprehensive list of analytical equations that can be used to determine aquifer parameters is listed in the text by Bruggeman (1999). The method developed by Carr and Van Der Camp (1969) is one of the earliest that is similar to the current application. In its application, the amplitude and the phase lag of tidally induced water levels were used to obtain aquifer characteristics. Pinder, et al. (1969) developed a method to determine aquifer diffusivity using aquifer response behavior under fluctuating river stages. Since analytical equations used for this method cannot be solved explicitly, best fit methods were needed to obtain diffusivity from this test. Recent work on canal-aquifer interaction by Zlotnik and Huang (1999) also involved analytical expressions for dynamic aquifer

response in the case of shallow penetrating streams with bed sediments. Additionally, Motz (2002) also obtained a solution for a leaky confined aquifer using a 1-D dynamic solution for a canal cross section. All these solutions were for sudden changes in canal levels. Lal (2001) obtained a solution for the canal-aquifer interaction problem assuming diffusion flow along the canal with sinusoidal water level changes. As a result of the solution, it was possible to identify dimensionless parameters important to the variation of water levels along the canal. Recent additions to methods capable of determining aquifer diffusivity include analytical methods developed by Swamee and Singh (2003) and Singh (2004). These approaches however require the use of optimization methods to determine parameters.

In the specific case of southeast Florida, understanding the Hydrogeology has been challenging from the beginning. The difficulties have been described by many investigators from earlier times as in the case of Klein, et al., (1977) to more recent times as in the case of Miller (1997). Many including Fish and Stewart (1991) have described the difficulty of characterizing the aquifer as confined or unconfined, and the difficulty of describing some of the properties. Recent investigators on the heterogeneity include Cunningham, et al. (2003). Under these difficult conditions, canal drawdown experiments in conjunction with flow meter experiments have been used in the past to determine aquifer parameters. Since conducting pump tests in southeast Florida has been found to be a futile task, most drawdown tests make use of steady state solutions to determine canal aquifer parameters. Chin (1991) for example developed an analytical method to determine aquifer transmissivity after considering the clogging effects of bottom sediments. This method has been tested in the L-31N canal. In this test, a term ”reach transmissivity” defined as the flow out of a canal per unit length per unit head drop is used to measure the composite aquifer and sediment resistance to seepage. Genereaux and Guardiaro (1998) also conducted a drawdown test based on steady state equations to determine aquifer and canal resistance properties in the L-31W canal. Most tests, based on a steady state assumption only provide a limited set of parameters related to canal-aquifer interaction.

In this study, analytical solutions for simulating the dynamics of fully coupled canal-aquifer

interaction at a canal cross section are developed. It is assumed that the system is disturbed through changes in the canal stage. The analytical expressions are used to understand important seepage characteristics and estimate aquifer parameters. The analysis is first carried out for a single Fourier component of a general solution in order to simplify it. The results of the analysis show the existence of a number of basic dimensionless parameter groups influencing the solution. Some of these groups were previously listed by Lal (2001). Furthermore, since this study is based on water level variations along the canal, it is difficult to focus on cross-section based behaviors. In the current study focusing on a cross section, the dimensionless parameter groups influencing the solution include (a) a parameter group related to aquifer diffusivity; (b) a parameter group explaining vertical leakance in the case of a confined aquifer; (c) a parameter group explaining canal sediment resistance; (d) a parameter group explaining canal and aquifer storages and aquifer transmissivity. These dimensionless parameter groups determine the propagation behavior in the aquifer and the water levels at any point in the system. Extreme behaviors such as the hydraulic cutoff between the stream and the aquifer are functions of these parameter groups.

Field tests were conducted in the L-31W canal, which is part of the managed south Florida conveyance system. During the test, periodic discharge disturbances of known magnitude were generated using pumps and structure facilities. Water level disturbance data collected during the test from various points in the system were used to calculate the phase and the amplitude of the disturbance. Explicit relationships between the wave characteristics and parameters were used to determine the parameter values for sinusoidal stresses. A dry period was preferred for the test due to the low noise level and the absence of ponding. A low noise level in the data was important as a way to reduce parameter uncertainty. The period of the wave was selected so that only the targeted zone adjacent to the canal was stressed.

Analytical expressions relating parameters to the stress-response relationships are useful when studying both physical and numerical systems. These analytical expressions can be used to solve a number of problems in system identification especially when there is excessive data noise and a lack of knowledge of cause-effect relationships between the stress and the response. In the current

experiment, both the stress and the response are sinusoidal and the calculations of parameters are based on measured amplitude and phase. Experiments such as this suggest that it is possible to determine targetted parameters of the system, or understand the effect of targetted parameters whether the system is physical or numerical. Understanding and calibrating numerical models is a novel use of these analytical expressions.

There are advantages and disadvantages associated with the test. It is generally environmentally nondestructive, and the effects are local. It is easier therefore to obtain approval of a test from regulating agencies, even when testing is conducted close to a sensitive area. The flexibility to select the frequency and the amplitude allows for control of the tested area. High frequency disturbances are useful for investigations close to th canal, and low frequency disturbances are useful for far field investigations. In both cases, the overall resolvability of the parameters is limited by data noise. The disadvantages of the test are mainly due to the difficulty of creating sinusoidal water level or discharge disturbances in canals using limited operational facilities. Disturbances that have square wave shapes are also useful, but the analyses are complex. The test assumes the absence of ponded water over the aquifer and the differences in water levels along the canal to be small compared with the amplitude. The test is proposed to many areas of South Florida where the canal segments are relatively short or the water level differences along the canal are small.

THEORETICAL CONSIDERATIONS

In this section, analytical expressions describing the dynamic behavior of canal-aquifer interaction are derived. The derivation is carried out for a canal cross section as shown in Figure 2 assuming that the canal is fully coupled with the aquifer, and the seepage is impeded by a possible canal sediment layer. Even if the analysis is carried out for a leaky confined aquifer, the results are applicable to both leaky and non-leaky confined aquifers as well as unconfined aquifers when the coefficient of leakage or leakance of the confining layer is set to zero. The water level is assumed to be flat, and therefore the results are applicable to many short canal segments in south Florida with structures at both ends. This assumption is valid when the water level differences along a canal are small compared to the water level changes in the canal over a test cycle. The following

analysis is aimed at obtaining expressions for aquifer parameters in terms of the amplitude and the phase of the water level at different points in the aquifer.

Influence of diffusivity and vertical leakiness on the propagation behavior of confined aquifers

The one dimensional governing equation for a leaky confined aquifer is used to derive expressions for two parameters; the aquifer diffusivity and the coefficient of leakage of the confining layer. The governing equation for groundwater flow in a semi-confined aquifer is (Bear, 1979)

$$s_c \frac{\partial H}{\partial t} - R = \frac{\partial}{\partial x}\left(T \frac{\partial H}{\partial x}\right) + \frac{k_v}{\delta_v}(h(t) - H) \tag{1}$$

in which $R =$ recharge per unit length; $T =$ aquifer transmissivity; $H =$ water head in the leaky confined aquifer; $h(t) =$ water head outside the leaky confined aquifer; $\delta_v/k_v =$ coefficient of leakage or leakance of the semi-pervious confining layer. In unconfined aquifers, transmissivity can be approximated as $T \approx K\bar{d}$ where $K =$ hydraulic conductivity; $\bar{d} =$ average aquifer depth. For fully confined and unconfined aquifers, the term with k_v/δ_v is absent. The analysis of (1) is based on a single Fourier component of the solution described as

$$\mathbf{H} = H_0 e^{If t - \mathbf{k}x} \tag{2}$$

where $f = 2\pi/P =$ angular frequency of the perpetual disturbance imposed on the systemas; $P =$ period of the disturbance; $\mathbf{k} = k_1 + k_2 I$ where $k_1 =$ amplitude decay constant; $k_2 =$ wave number and $I = \sqrt{-1}$. All complex numbers are in boldface.

Values of k_1 and k_2 are key to the determination of aquifer parameters such as diffusivity (Carr and Van Der Camp, 1969). They are determined experimentally using linear plots of log amplitude and phase lag with distance at different points in the path of propagation. The linear equations used for this purpose are derived using (2) which can also be stated as $H_2 = H_0 e^{-k_1 x}\sin(ft - k_2 x)$. The linear equations are:

$$-\ln\left(\frac{|\mathbf{H_2}|}{|\mathbf{H_0}|}\right) = k_1\, x - \ln(\alpha_s) \tag{3}$$

$$\varphi = k_2\, x + \varphi_s \tag{4}$$

in which, $H_0 = |\mathbf{H_0}| =$ amplitude of the water level at the canal; $H_2 =$ amplitude of the water level at a distance x from the canal; $\alpha_s =$ ratio of the amplitude of the water level just outside the canal

sediment layer to the amplitude in the canal; φ = phase lag between the water level in the canal and a point at a distance x from the canal; φ_s = sudden change in the phase due to canal sediment. The graphs of $-\ln(|\mathbf{H_2}|/|\mathbf{H_0}|$ vs x and φ versus x for a homogeneous medium are straight lines with slopes k_1 and k_2 respectively. Both α_s and φ_s can be calculated from the intercepts. If there is no sediment layer, the intercept would be zero. Any nonlinearity in the curve indicates inhomogenuity of the aquifer with local slopes reflecting local parameters.

In the case of fully confined aquifers, $k_1 = k_2 = k_0$ (Carr and Van Der Camp, 1969). When the aquifer is semi-confined, k_1 and k_2 deviate from each other. The amount of deviation of k_1 and k_2 from a base value of k_0 for non-leaky aquifers can be used to obtain the coefficient of leakage itself. In order to calculate an expression for measuring the coefficient of leakage, (2) is substituted in the governing equation (1), and the result $\mathbf{k^2} = 2(I+\eta)k_0^2$ is solved to give $\mathbf{k} = k_0 n(\eta)\exp(I\kappa)$ in which.

$$n(\eta) = \sqrt{2}(1+\eta)^{\frac{1}{4}} \tag{5}$$

$$\kappa(\eta) = \tan^{-1}\frac{1}{(\sqrt{1+\eta^2}+\eta)} \tag{6}$$

$$k_0 = \sqrt{\frac{s_c f}{2T}} \tag{7}$$

$$\eta = \frac{1}{s_c f}\frac{k_v}{\delta_v} \tag{8}$$

When expressed as real and imaginary components of $\mathbf{k}$,

$$k_1 = k_0\sqrt{\left(\sqrt{1+\eta^2}-\eta\right)}(\sqrt{1+\eta^2}+\eta) \tag{9}$$

$$k_2 = k_0\sqrt{\left(\sqrt{1+\eta^2}-\eta\right)} \tag{10}$$

The dimensionless parameter η in (8) describes the leakiness of a confined aquifer. The equations show that $k_1 = k_2 = k_0$ for confined aquifers, and $k_1 > k_2$ when the confined aquifer becomes leaky. If k_1 and k_2 are significantly different, the implication is the presence of a leaky semi-confining layer. In this case (9) and (10) can be used to determine η by first calculating $r_k = k_1/k_2 = \eta + \sqrt{1+\eta^2}$ and then using $\eta = 0.5(r_k^2-1)/r_k$. Parameter k_0 is then computed using

$k_0 = \sqrt{(k_1^2 + k_2^2)}/n$. For unconfined aquifers or fully confined aquifers with no leakiness, $\eta = 0$, $n(\eta) = n = \sqrt{2}$, and $k_1 = k_2 = k_0$. If there are enough data and the slopes k_1 and k_2, along with their intercepts vary from place to place in the aquifer, the values can be used to create a map of aquifer properties can be plotted on a map to show the heterogenuity.

If the aquifer is leaky confined, $k_1 > k_2$ implying that disturbances decay faster and travel slower. If for example a difference between k_1 and k_2 of more than 5% is considered detectable and significant, the condition for a confined aquifer becoming leaky can be expressed as $\eta > 0.05$. Similarly, if the difference is more than 25%, then $\eta > 0.25$. When the leakiness is extremely large and k_2 reduces to a very low value such as 5% of its original value, the corresponding $\eta \approx 200$. The disturbances decay very rapidly under this condition. The governing equation (1) with an extremely large leakage term is not practically useful.

Numerical experiment to verify the analysis

A numerical experiment was carried out using the MODFLOW model (McDonald and Harbough, 1988) to test the validity of equations (9) and (10). In the experiment, real and imaginary components of **k** obtained using the analytical expressions and the MODFLOW model were plotted separately as shown in Figure 3. For the MODFLOW model, a 1-D two layer groundwater problem was set up with 200 cells of 100 m length. The confined layer was assigned a transmissivity value of $2.777 \times 10^{-4}\ m^2/s$ and a storage coefficient of 0.001. A sinusoidal pumping rate with a period of $P = 48$ Hrs or $f = 3.636 \times 10^{-5}\ s^{-1}$ was used with an amplitude of $1.0\ m^3/s$. Water levels at distances of 100 m, 200m, and 300 m were observed at every 1.0 Hr time step. The model was run with values of k_v/δ_v ranging between $5.5 \times 10^{-12}\ s^{-1}$ and $1.0 \times 10^{-7}\ s^{-1}$. The amplitude and the phase of the observed water level disturbance were calculated using the least square method as described later. The amplitudes were used to calculate k_1 using (2) giving $k_1 = \ln(H_2/H_1)/(x_2 - x_1)$ where H_1 and H_2 are the amplitudes at observation stations 1 and 2 at distances x_2 and x_1 from the canal. Phase measures were used to calculate k_2 using $k_2 = \phi_2 - \phi_1/(x_2 - x_1)$ where ϕ_1 and ϕ_1 are the phase values at stations 1 and 2. The value of k_0 was computed as descried earlier as 8.09 $\times 10^{-3}\ m^{-1}$. Figure 3 shows that the values of k_1/k_0 and k_2/k_0 obtained using the MODFLOW

model agree with the analytical solution. The figure also shows how the speed of propagation decreases and attenuation increases with increasing leakiness.

Analytical relationship for water levels across the sediment layer

If the intercepts in (3) and (4) are not zero, values of α_s and φ_s obtained from these intercepts can be used to calculate the parameters related to the canal sediment layer. The following mass balance condition is used to obtain equations relating the intercepts to the parameters.

$$-T\frac{\partial H_1}{\partial x}|_{x=0} = p\left(\frac{k_s}{\delta_s}\right)(H_0 - H_1) \tag{11}$$

where $p =$ wetted perimeter along which seepage occurs; $k_s =$ hydraulic conductivity of the sediment layer; $\delta_s =$ thickness of the sediment layer; $k_s/\delta_s =$ leakage coefficient of the canal sediment layer. Figure 2 shows a definition sketch. If there is heterogeneity of sediment properties at the bottom or the sides, a composite value of pk_s/δ_s has to used. Assuming the solution in the canal is described as $\mathbf{H_0} = H_0 e^{Ift}$, and the solution in the aquifer just outside the sediment layer is described as $\mathbf{H_1} = H_1 e^{Ift - I\varphi_s}$, the following can be obtained using (11) after simplification.

$$T\mathbf{k}\mathbf{H_1} = p\frac{k_s}{\delta_s}(\mathbf{H_0} - \mathbf{H_1}) \tag{12}$$

After substituting for $\mathbf{k}$ from previous section, this reduces to

$$\left[\frac{n(\eta)}{\sigma}e^{\kappa I} + 1\right]\mathbf{H_1} = \mathbf{H_0}e^{-I\varphi_s} \tag{13}$$

where $\sigma =$ dimensionless sediment conductance parameter defined as (Lal, 2001)

$$\sigma = \frac{p}{Tk_0}\frac{k_s}{\delta_s} = p\frac{k_s}{\delta_s}\sqrt{\frac{2}{fs_cT}} \tag{14}$$

Equation (13) can be used to express the relationship between $\mathbf{H_1}$ and $\mathbf{H_0}$ as

$$\mathbf{H_1} = \frac{\sigma\, e^{-I\varphi_s}}{\sqrt{n^2 + 2n\sigma\cos\kappa + \sigma^2}}\mathbf{H_0} \tag{15}$$

Equation 15 shows that the amplitude $\mathbf{H_0}$ is reduced due to the sediment layer by a factor α_s given by

$$\alpha_s(\sigma,\eta) = \frac{\sigma}{\sqrt{n^2 + 2n\sigma\cos\kappa + \sigma^2}} \tag{16}$$

and the phase lag due to the sediment layer is

$$\varphi_s(\sigma,\eta) = \sin^{-1}\frac{n\,\sin\kappa}{\sqrt{n^2+2n\sigma\cos\kappa+\sigma^2}} \tag{17}$$

If the aquifer is unconfined or non-leaky confined, $n=\sqrt{2}$ and the reduction of amplitude due to the canal sediment layer alone can be shown to be varying with σ as described in Figure 4. According to this figure, the canal is at a completely cutoff state (5% connection) when $\sigma < 0.073$ and a completely connected state (95% connection) when $\sigma > 19.5$. Table 1 shows a summary of this and other dimensionless parameters.

Relationship between a flow pulse and the resulting head response

The following mass balance equation for a unit length of the canal is used to obtain a relationship for the change in water level in a canal for a given inflow.

$$q + 2T\frac{\partial H_1}{\partial x} = B\frac{\partial H_0}{\partial t} \tag{18}$$

in which, $q=$ discharge into the canal per unit length; $H_0=$ water level in the canal; $B=$ width of the canal. Substituting the sinusoidal form of the solution discussed earlier for water level, and using $\mathbf{q} = q_0 e^{Ift+I\theta}$ for discharge rates, the following expression can be obtained after using (15) to explain the relationship between H_1 and H_0.

$$\frac{q_0}{fB}e^{-I\varphi_s} = H_0\left[\frac{\sqrt{2}\alpha_s(\sigma)\,n(\eta)}{\chi}e^{(\kappa-\varphi_s)I}+I\right] \tag{19}$$

in which χ is the single most important dimensionless parameter describing both storage and resistance effects of canal-aquifer interaction.

$$\chi = \frac{fB}{\sqrt{2}Tk_0} = B\sqrt{\frac{f}{Ts_c}} \tag{20}$$

The effects of the sediment layer and the coefficient of leakage of the aquifer also influence the solution. These effects can be incorporated into χ in (19) using the modification

$$\chi' = \chi\frac{\sqrt{2}}{\alpha_s(\sigma)\,n(\eta)} \tag{21}$$

in which $\alpha_s(\sigma)$ is defined using (16) and $n(\eta)$ is defined using (5). In unconfined or non-leaky confined aquifers, $\chi' = \chi/\alpha_s(\sigma)$. If there is no sediment resistance as well, $\chi' = \chi$.

The ratio of the change of head to the change of flow can be defined as a dimensionless parameter ξ. This parameter can be described using (19) as

$$\xi(\chi,\sigma,\eta) = \frac{H_0 fB}{q_0} = \frac{\chi'}{\sqrt{(4+(\chi')^2+4\chi'\sin(\kappa-\varphi_s))}} \tag{22}$$

The phase lag θ between the head and the discharge can also be obtained using (19) as

$$\theta(\chi,\sigma,\eta) = \cos^{-1}\left\{\frac{2\cos(\kappa-\varphi_s)}{\sqrt{(4+(\chi')^2+4\chi'\sin(\kappa-\varphi_s))}}\right\} \tag{23}$$

Equations (22) and (23) are similar to (16) and (17) in behavior. If there is no aquifer to interact, $\xi = 1$. If it is assumed that the interaction is negligible at $\xi > 0.95$, the corresponding condition is $\chi' > 27.6$. The canal amplitude is maximum under this condition. Similarly the interaction is maximum and there is significant damping of canal amplitude with $\xi < 0.05$ or $\chi' < 0.1$. Figure 5 shows the two cutoff values of 95% and 5% at both ends of the asymptotic curve. If the effect of the sediment layer is insignificant, $\sigma = 0$, and therefore $\varphi_s = 0$, $\alpha_s(\sigma) = 1$ and $\chi' = \chi$. Equation 22 then reduces to

$$\xi = \frac{H_0 fB}{q_0} = \frac{\chi}{\sqrt{2+(\sqrt{2}+\chi)^2}} \tag{24}$$

which relates the pulse response behavior to aquifer property χ.

The parameters χ and k_0 together are useful in obtaining primitive values of T and s_c. The parameter k_0 only gives the diffusivity T/s_c and χ gives Ts_c. They both have to be combined to obtain T and s_c

Numerical experiment to verify the analysis

Numerical experiments were carried out to determine the validity of (22) and (23) and understand relationships among relevant dimensionless variables. A 1-D fully implicit numerical model having a formulation similar to MODFLOW was used for this purpose with spatial and temporal discretizations of 100 m and 1hr respectively. In the model, a canal subjected to water level disturbances of period 16 hrs was simulated. Other model parameters were selected to give decent ranges for the dimensionless parameters investigated. The results shown in Figures 5 and 6 are independent of the actual physical dimensions of the problem. These results show how ξ and θ

vary with χ and σ. The solid line shows analytical values and the symbols show numerical model values. The results show that the numerical solution agrees with the analytical solutions.

Numerical experiment showing the applicability of the analytical solution to short canals

The analytical solutions derived in this paper are exact for infinitely long straight canals. Unfortunately some canals in South Florida are short. In this section, the applicability of the solution to short segments is tested by comparing the numerical solution in a 2-D model domain with the analytical solution. The complete analytical solution for a short segment is obtainable by superimposing point solutions of variable strength. This method that is not presented here, forms the basis of the transient analytic element method for Dupuit-Forchheimer flow (Bakker, 2004).

The numerical solution of the test problem used for the test is shown in Figure 7. It is obtained using the RSM model (Lal, et al. 2005) with a right triangular mesh of size 10 m and canal discretization of length 100 m. It shows dimensionless water levels around the closed end of a short canal. The distances used in the figure are in dimensionless units, created by dividing the actual length by a characteristic length $\lambda = \sqrt{T/(fs_c)}$. The contours of the amplitudes of ground water levels obtained numerically are plotted as a fraction of the amplitude of water level at the canal (H/H_0). The other parameters used in the experiment are: $P = 32$ Hrs, $T = 0.003\, m^2/s$ and $s_c = 0.2$. The sediment layer is assumed to be absent making $\alpha_s = 1.0$ and $\varphi_s = 0$. For the parameters selected, the characteristic length is $\lambda = 16.58\, m$. In order to obtain an analytical solution to compare with the numerical solution, the parameter χ is computed first as $\chi = 5.52$ using (20) and $B = 18.3\, m$. The dimensionless amplitude of the water level fluctuation is calculated next using (22) as $\xi = 0.78$. The corresponding dimensional value is $q_0 = 0.01$ as $H_0 = q_0\xi/(fB) = 7.81m$. For comparison, the numerical model result obtained using the RSM model shown in Figure 7 is 7.56 m. The difference between these values have to do more with the crude discretization. This experiment shows that (22) is a good approximation even for shorter canal segments.

The amplitudes of groundwater levels obtained analytically and numerically at an arbitrary distance of 20 m from the center of the canal are also compared next. The analytical solution computed using (2) and (8) is $H_y = H_0 \exp(-y/(\lambda\sqrt{2}))$. At a distance $y = 20m$, $H_y = 7.81 \times$

$\exp(-20/(16.58\times\sqrt{2})) = 3.32$ m. The value obtained using the RSM model, as shown in Figure 7 is 3.15 m. These results show that unless the canal is extremely short, the numerical solutions for groundwater and canal flow are reasonably close to the analytical solutions. Considering that the discretization is crude, the discrepancy has more to do with the numerical error.

Methods used to obtain the amplitude and the phase from time series data

The first step toward determining aquifer parameters involves analyzing the water level time series data to obtain the amplitudes and the phase lags. A number of techniques are available to carry out this task. Since the frequency of the disturbance is constant during the experiment, the problem involves the determination of amplitude a and the phase b when the data are fitted to $H = a\ \sin(ft + b)$. Before fitting to the curve, the data are de-trended to remove any regional influences. After that, three methods were used to obtain a and b values.

The first method used to calculate a and b is based on a least square best fit approach. This method can be used even with missing or short data records. With this approach, S is minimized for elapsed times t_i in which $i = 1, 2, \ldots n_t$; $n_t =$ number of time records.

$$S = \sum_{i=1}^{n} (Y_i - a\sin(ft_i + b))^2 \tag{25}$$

Conditions $\frac{\partial S}{\partial a} = 0$ and $\frac{\partial S}{\partial b} = 0$ give the following to be solved for a and b

$$\frac{\sum Y_i \sin(ft_i + b)}{\sum \sin^2(ft_i + b)} - \frac{\sum Y_i \cos(ft_i + b)}{\sum \sin(ft_i + b)\cos(ft_i + b)} = 0 \tag{26}$$

$$\frac{\sum Y_i \sin(ft_i + b)}{\sum \sin^2(ft_i + b)} = a \tag{27}$$

The second method is based on the cross correlation of the de-trended data. The phase lag and the ratio of the amplitudes that give the best correlations are selected as b and a respectively. A third approach was also used based on manually selected peak and trough points in the water level curve. The amplitude and the phase lag calculated manually are crude. However this last method can eliminate some known data problems.

APPLICATION TO THE L-31W TEST SITE

A pilot tetst was conducted in the L-31W canal in South Florida to see if the analytical expressions derived earlier can be put to practical use. This is accomplished by using them to understand the dynamics of the canal-aquifer system and calculate bulk aquifer parameters. The test can also teach lessons for future tests.

Description of the site and the test

The test site selected is the 11.5 km stretch of the L-31W canal in South Florida between structures S-174 and S-175. The L-31W canal built around 1971 is located in Dade County, FL, along the Eastern boundary of the Everglades National Park. The L-31W canal penetrates the extremely pervious surficial aquifer called the Biscayne aquifer. This aquifer is the most prolific aquifer in Dade County and contains highly permeable sands and limestones (Fish and Stewart, 1991). It is approximately 14 m thick near the canal, with the top 1/3 rd. made of marine limestone, and the bottom 2/3 rd. is referred to as the Ft Thompson formation. The ground elevation in the area is around 1.2 m - 1.8 m.

The test was started on 02/21/2003 at 0:00 Hrs with the rising phase of the cycle and lasted until 02/26/2003. During the test, sinusoidal water level disturbances of period $T_p = 48$ Hrs were created in the canal by using a structure S-174 in the North and S-175 in the south. The pumps and structures allowed a maximum flow rates of around 5 m^3/s in and out of the canal. The 48 Hr period allowed for a large enough amplitude, and avoided possible conflicts with the tidal cycles. Even if a large number of sine cycles would have been ideal, it had to be limited to a few in order to minimize the interference with the daily operation and management of the Everglades National Park and the south Florida conveyance system.

Summary of test results

A summary of test results at various stages of the calculation process is shown below. Figure 8 shows the raw water levels at the canal and a number of selected gages. It shows the influence of the test superimposed on the regional system behavior. The figure also shows the effect of a small rainfall measured at gage R127 on water levels. Figure 9 shows the detrended discharge and water level data, and the curves fitted to the data using the least square method described in (26)

and (27). The figure shows that water level in the aquifer varies smoothly when compared with pumping rate variation indicating that the aquifer is capable of smoothing many of the high frequency fluctuations. The noisy pumping rate is an indication of the effort made by the operators to maintain the sinusoidal water level targets. Some of the extremely noisy periods of the record were not used in the analysis. Table 2 shows the summary of the sinusoidal curve fits obtained using the three methods explained earlier. Statistical estimates associated with the fit are also shown. Some of these estimates may be used to determine the uncertainties of the parameters.

Transmissivity and vertical leakance near L-31W

Amplitude and phase characteristics of the sinusoidal water levels measured at different points in the aquifer are used to calculate transmissivities and vertical leakances of the aquifer. Table 2 shows the amplitudes and phases which are used to plot $-\log(H/H_c)$ versus x and φ_s versus x curves described in (3) and (4). Figures 10 and 11 show the plots. Table 3 shows the estimates of k_1 and k_2 obtained using the slopes. The results show $k_1 > k_2$ indicating the presence of a confining layer. The values of k_1 and k_2 are used to obtain η and k_0 as described earlier. They can be used to determine the aquifer diffusivity and the vertical leakance. If data are available for many gages, spatial distribution of the same properties can be plotted. Table 4 shows dimensionless parameter values obtained for L-31W.

Bottom sediment properties if L-31W

Effects of canal sediment resistance can be detected by the presence of intercepts in the $-\log(H/H_0)$ versus x curve and the φ_s versus x curve. Figures 10 and 11 both show the presence of this resistance. Since the functional relationship between σ and the intercept is known, the intercepts in (3) and (4) can be used to determine σ using (16) and (17). Table 4 shows the values of σ obtained for L-31W using the intercepts of (3) and (4).

Aquifer and canal storage properties of the L-31W surroundings

Storage parameters related to stream-aquifer interaction are determined using the amplitude and the phase lag of the discharge and the water level in (22) and (23). Using (22), the value of ξ can be calculated based on data in Table 2 as $\xi = H_0 fBL/Q_0 = 0.193 \times 3.636 \times 10^{-5} \times 18.3 \times 11500/5.805 = 0.254$. The value of χ' can now be solved using (22) as $\chi' = 0.54$. The value of χ'

can also be solved using (23) by first calculating phase $\theta =$ as 0.69 and then solving $\chi' = 1.44$. In order to calculate χ from the value of χ', equation $\chi = \chi' \alpha_s(\sigma)\ n(\eta)/\sqrt{2}$ is used. The parameter values used for this are $\alpha_s(\sigma) = 0.65$ and $n(\eta) = 2.0$. The final values of $\chi = 0.5$ and $\chi = 1.33$ are also shown in Table 4.

Table 4 shows the dimensionless parameters obtained for the overall L-31W system and the NTS1 zone. Table 5 shows the dimensional parameters. The uncertainty estimates of some of these parameters can be obtained using the standard error estimates in Table 2 if necessary.

Primitive variables of the L-31W surrounding

Dimensionless parameter groups obtained from the experiments can be used to calculate primitive variables. Primitive variables T ans s_c for example are calculated using T/s_c and Ts_c obtained from k_0 and χ. Using the least square method, it is possible to obtain $k_0 = 2.47 \times 10^{-4}$ as shown in Table 4. Aquifer diffusivity determined using k_0 is $T/s_c = \sqrt{f/(2k_0^2)} = 297\ m^2/s$ because $f = 3.636 \times 10^{-5}\ s^{-1}$. The value of $\chi = 0.50$ can be used with the definition (20) to calculate $Ts_c = B^2 f/\chi^2$ or $18.3^2 \times 3.636 \times 10^{-5}/0.50^2$ making $Ts_c = 0.0742\ m^2/s$. Combining with the value of diffusivity, it is possible to obtain $T = 4.49 m^s/s$ and $s_c = 0.0158$. Other primitive variables calculated in this manner are shown in Table 5.

DISCUSSION

Inaccuracies and problems with the field test and implications of the results are discussed in this section. The first type of inaccuracy discussed is due to ground surface features such as sloughs and agricultural ditches that influence the behavior of near-surface groundwater flow. Taylor slough shown in Figure 1 is a good example for a surface feature influencing the high water levels of E112. Figure 8 shows the artificially low amplitude of E112 resulting from water seepage out of the system during the high phase of the cycle. The same is true with gages in the Frogpond agricultural area because of the network of drainage canals that diffuse the high water levels in the cycles. Table 2 shows the amplitude data while Figures 10 and 11 show all the data in one plot. The figures show that some of the data anomalies. Experience with the test shows that identifying the affected gages closer to a wetland is not an easy task.

The second type of error discussed here is caused by unpredictable incidents of highly variable local rainfall affecting the water level as shown in Figure 8. In the current analysis, these effects are considered as data noise to make the analysis simple. A third error is due to the noise in the flow data when pumps and structures are used during operations aimed at maintaining target water levels. There are times when the structures and pumps had to be operated close to or beyond peak capacities almost clipping the peaks and troughs of the cycle.

Table 2 shows that the amplitude and phase characteristics of the collected data depend on the method of calculation. The table shows that data are clean for a number of gages that are not too far from the canal. For some of the gages, the standard errors are large compared to the amplitudes making them less useful. With and without error bars shown in Figures 10 and 11, knowledge about the scatter is useful in visually evaluating the quality of the data at various gages. Figures 10 and 11 also show that it is possible to obtain good straight line fits. Results in Table 3 indicate that the slopes, intercepts and aquifer properties vary from zone to zone.

Tables 4 and 5 also show the spatial variability of the properties around the canal. Results of a single test zone close to NTS1 and NTS10 are presented in this paper. The variability of the properties in the table can be attributed to the heterogeneity of the limestone aquifer in addition to errors in the data. The short duration of the test also has an effect on the accuracy of the results.

The second row of Table 5 shows the diffusivity computed assuming that the aquifer is not leaky. This is a simplifying assumption used by Carr and Van Der Camp (1969). They refer to the diffusivity computed using the amplitude as the effificncy based diffusivity. For the NTS1 zone, the value obtained is 132 m^2/s. For the same zone, the diffusivity computed using phase lag is 5233 m^2/s. The difference in diffusivities have also been observed by Smith and Hick (2001) and others as well. In the current analysis, this difference is explained using the leakiness in the confined aquifer. This result has a strong implication on groundwater model development. It show that if a leaky confined aquifer is modeled using a single layer confined aquifer or a single layer unconfined aquifer, the solution will be out of phase if the amplitudes match, or the solution will

have different amplitudes if the phases match.

The results of the test shown in Table 5 can be used to demonstrate the practical use of (8). For example, if it is necessary to determine the time scale of a transient problem near L31-W for which the confining layer becomes non-leaky for all practical purposes, a condition such as $\eta < 0.25$ can be used assuming a difference of less than 25% between k_1 and k_2 to be the deciding factor. This condition can be expressed as $(k_v/\delta_v)P/(2\pi s_c f) < 0.25$. With numbers from the table, $0.25 > 0.0315P/(2\pi \times 0.0158)$ gives $P < 0.8$ days. This means there is a need to have a second confined layer in a computer model when the water level fluctuations have a period shorter than 0.8 days. This also implies that the system can be considered as unconfined for all practical purposed when carrying out regional model applications with time steps larger than 1 day.

Looking at the results in Table 4 and Table 5, it is clear that water level and time data for field experiments have to be collected fairly accurately for the error to be reduced. It is also important to have as many gages are spatially spread in order to obtain the spatial distribution of diffusivity. Aquifer diffusivity is the most reliable property that can be calculated from the experiment because it is based only on the water level. However when other properties have to be calculated, there is only one discharge data set available for the purpose. This results in giving only one value of Ts_c for the entire canal segment. The individual values of T and s_c computed in this manner for a heterogeneous aquifer are less reliable because the computed values of T/s_c are local and computed values of Ts_c are regionally averaged.

Results of drawdown experiments carried out in the past in the L-31W area and the nearby L-31N area show a significant variability of the parameters. Fish and Stewart (1991) showed that the values of transmissivity can be as high as 1.8 m^2/s in the area and reaching 3.2 m^2/s near Krome Avenue close to Miami. Chin (1991) obtained values close to 1.3 m^2/s near L31-N. Genereaux and Guaridiaro (1998) observed a value close to 1.2 m^2/s for the Byscayne aquifer and $k_s/\delta_s = 35.2$ day^{-1} for the coefficient of leakage of the sediment. Results of multi-well aquifer tests reported by Reese and Cunningham (2000) suggest $T = 0.1m^2/s$, storativity= 0.0004 and $k_v/\delta_v = 0.007$

day^{-1} at Trail Center that is 50 km northwest of the site. Model calibration has also been used to obtain parameters. Nemeth, et al. (2000) obtained $s_c = 0.0002$, $k_v/\delta_v = 78\ day^{-1}$, $T = 1.5\ m^2/s$ using the MODBRANCH model.

SUMMARY AND CONCLUSIONS

The governing equations were analyzed to understand the dynamic behavior of a fully integrated canal-aquifer system. Results of the analysis include analytical expressions describing the response of the system to sinusoidal discharge stresses. Using the results, experimental methods were developed to help determine physical parameters of the system. When the analytical expressions were tested using numerical models applied to a number of test problems, the results show agreement. Dimensionless parameters that influence various processes were also identified using the equations. Table 1 shows a summary of the basic dimensional parameter groups responsible for various processes related to stream-aquifer interaction. Ranges of parameters controlling various processes are also shown in the table.

The dimensionless physical parameter groups that contribute to or explain various processes include η for leakage of the confined aquifer, σ for sediment resistance and χ for canal-aquifer storage relationship. Other parameters used to describe the system behavior include ξ for the response of the head in the canal to a given flow impulse. The analytical solutions needed to explain canal-aquifer interaction are explained in this paper for the case of sinusoidal stresses.

Results of the analysis show that aquifer leakance expressed in dimensionless form using η influences the propagation behavior. A curve showing the influence of η on the phase and the attenuation can be used to obtain a condition such as $\eta > 0.05$ for which an aquifer can be considered leaky confined for practical purposes, when detected at a 5% level. Results of the propagation behavior obtained using the MODFLOW model and the analytical expression are plotted against η showing that they agree. If η is very large, an aquifer system cannot be simulated numerically using just one layer alone. If only one layer is used, calibration cannot match both the phase and the amplitude of the solutions at the same time.

The analytical results show that for fully confined or unconfined aquifers, the canal can be completely cutoff from the aquifer due to sediment alone regardless of aquifer properties if $\sigma < 0.073$. Under such cutoff conditions, the canal and the aquifer can be considered moving independently. The same condition $\sigma < 0.33$ was obtained by Lal (2001) after studying the variation of longitudinal water levels along a canal. At the opposite end of cutoff, a canal is completely connected if $\sigma > 19.5$ assuming a detection level of 5%.

The analytical results also show that in addition to the sediment effects, canal can be completely cutoff because of aquifer properties and canal storage effects too, if $\chi' > 27.6$. In a previous study of longitudinal fllow profiles by Lal (2001), the same condition was obtained as $\chi' > 10$. At the opposite end of cutoff, the canal is completely connected to the aquifer and the canal and aquifer water levels are the same if $\chi' < 0.1$.

A separate test problem was used to investigate the applicability of the analytical method to relatively short segments. Using the test it was able to demonstrate that the analytical expressions derived for long canals can be used for fairly short canals as well. In carrying out the test, the flow around a short segment was solved numerically using both the RSM model and the analytical methods. The results show that the numerical results agree closely with the analytical solution even when the canal is relatively short.

Practical applications of the analytical methods developed in this paper include primarily the calibration of field parameters associated with canal-aquifer interaction. A second use of the equations is to assist in the calibation of numerical models by providing an exact solution for the numerical solution to be compared against. An application of this approach would involve carrying out a field test to determine the parameters first, and using the parameters in the numerical model to be compared against both the field data and the analytical solution.

ACKNOWLEDGEMENTS

The author wishes to acknowledge Joel Van Arman, Mark Wilsnack, Todd Tisdale, Steven Krupa, Cynthia Gefvert, for reviewing the manuscript, Ron Mierau, George Hwa, Cal Neidrauer and Paul Linton of the South Florida Water Management District for supporting and carrying out the test on a busy conveyance system, and Clay Brown for the GIS help. He also wishes to thank Kevin Kotun and others of the Everglades National Park, USACOE and the USFWS for their support of thee test, and the peers Randy Van Zee, Ken Konyha for healthy comments.

REFERENCES

Bakker, M. (2004). "Transient analytic elements for periodic Dupuit-Forchheimer flow", *Adv. Water Resources*, (27), 3-12.

Bear, J. (1979). *Hydraulics of groundwater*, Mc Graw-Hill, New York, NY.

Bruggeman, G. A. (1999). *Analytical solutions of geohydrological problems, developments in water science*, vol 46, Eq 228.01, Elsevier Publishers, Amsterdam.

Carr, P. A. and Van Der Kamp, G. S. (1969). "Determination of aquifer characteristics by the tidal method", *Water Resources Research*, 5(5), 1023-1031.

Chin, D. A. (1991). "Leakage of clogged channels that partially penetrate surficial aquifers", *J. Hydraul. Eng.*, 117(4), 487-488.

Cunningham, K. J., Carlson, J. L., Wingard, G. L., Robinson, E., and Wacker, M. A. (2004). "Characterization of Aquifer Heterogenity Using Cyclostratigraphy and Geophysical Method in the Upper Part of the Karstic Biscayne Aquifer, Southeastern Florida", *Water Resources Investigations Report 03-4208*, USGS.

Fish, J. E. and Stewart, M. (1991). *Hydrogeology of the surficial aquifer system*, USGS water resources investigation report 90-4108.

Genereaux, D. and Guadiario, J. (1998). "A canal drawdown experiment for determination of aquifer parameters", *J. Hydrologic Engrg.*, ASCE. 3(4), 294-302.

Klein, H., Armbruster, J. T., McPhearson, B. F., Freiberger, H. J., (1977). "Water and the south

Florida environment", *USGS Water resources investigation* 24-75, p-165.

Lal, A. M. W. (1998). "Calibration of riverbed roughness",

Lal, A. M. W. (2001). "Modification of canal flow due to stream-aquifer interaction", *J. Hydraul. Eng.,* 127(7), 567-576.

Lal, A. M. W., Van Zee, R. and Belnap, M. (1995) "Case Study: Model to Simulate Regional Flow in South Florida", *J Hydraul. Eng.,* 131(4), 1-12.

McDonald, M. G. and Harbaoug, A. W. (1988). "A Modular three dimensional finite difference groundwater flow model", US Geological Survey Techniques of Water Resources Investigations, Book 6, Reston, VA.

Miller, J. A. (1997). *Hydrogeology of Florida* in Randazzo, A. F., and Jones, D. S., The geology of Florida, Chapter 6, University of Florida press, Gainesville, FL., 69-88.

Motz, L. H. (2002). "Leaky one-dimensional flow with storage and skin effect in finite width sink", *J. Hydraul. Engr.,* 128(5), 298-304.

Drawdowns for leaky-aquifer flow with storage in finite width sink", *J. Hydraul. Eng.,* 120(4), 820-827.

Nemeth, M. S., Wilcox, W. M., Solo-Gabriele, H. M., Evaluation of the use of reach transmissivity to quantify leakage beneath levee L-31N, Miami Dade County, FL, USGS Water Resources Investigations Report 00-4066

Pinder, G. F., Bredehoeft, J. and Cooper, H. H. (1969). "Determination of aquifer diffusivity from aquifer response to fluctuations in river stage", *Water Resources Research,* 5(4), 850-855.

Reese, R. S. and Cunningham, K. J. (2000). "Hydrogeology of the gray limestone aquifer in Southern Florida", *USGS Water Resources Investigations Report 99-4213,* 51-59.

Singh, S. K. (2004). "Aquifer response to sinusoidal or arbitrary stage of semipervious stream", *J. Hydraul. Engrg.,* 130(11), 1108-1118.

Smith, A. J. and Hick, W. P. (2001). "Hydrogeology and Aquifer Tidal Propagation in Cockburn

Sound, Western Australia", *CSIRO Land and Water*, Technical Report 6/01, February 2001.

Swamee, P. K. and Singh, S. K. (2003). "Estimation of aquifer diffusivity from stream stage variation", *Journal of hydrologic engineering*, January/February, 20-24.

Zlotnik, V. A. and Huang, H. (1999). "Effect of shallow penetration and streambed sediments on aquifer response to stream stage fluctuations", *Groundwater*, 37(4), 599-604.

NOTATION

The following symbols were used in the paper.

B	width of the canal, (m).
f	angular frequency, (s^{-1}).
$h(t)$	water level in the overlying phreatic aquifer, (m).
H	water head in the aquifer, (m).
H_0	water level in the canal, (m).
H_1	water level just outside the canal and the sediment layer, (m).
H_2	water head in the aquifer, (m).
k_0	value of k_1 and k_2 for fully confined aquifers, (m^{-1}).
k_1	amplitude decay constant, (m^{-1})
k_2	wave number (m^{-1})
k_s/δ_s	coefficient of leakage of the sediment layer, (s^{-1})
k_v/δ_v	coefficient of leakage or leakance of the semipervious confining layer, (s^{-1})
p	wetted perimeter, (m)
P	period of the disturbance
q	discharge into the canal per unit length, (m^2/s)
R	1-D aquifer recharge per unit length, (m/s)
α_s	reduction of amplitude at the sediment layer
s_c	storage coefficient of the aquifer
T	transmissivity of the aquifer, (m^2/s)
η	dimensionless parameter describing the leakiness of the aquifer
λ	characteristic length of the aquifer, (m)
σ	dimensionless sediment conductance parameter
χ	dimensionless parameter describing resistance and storage effects of canal-aquifer interaction
χ'	parameter χ modified by the sediment layer and the leakiness
φ	phase lag at a distance x from canal
φ_s	sudden phase lag due to canal sediment
ξ	dimensionless parameter describing change in head per change in discharge

TABLES

Table 1: Summary of important parameters and their ranges

Description of the parameter and the range	expression
Parameter describing vertical leakiness of the confined aquifer η: aquifer is confined if $\eta < 0.05$ and extremely leaky confined if $\eta > 100$	$\eta = \frac{1}{s_c f}\frac{k_v}{\delta_v}$
Wave number and log decay rate in a fully confined or an unconfined aquifer	$k_0 = \sqrt{\frac{s_c f}{2T}}$
Wave number in a leaky confined aquifer $k_2 < k_0$	$k_2 = k_0\sqrt{(\sqrt{1+\eta^2}-\eta)}$
Decay constant in a leaky confined aquifer $k_1 > k_0$	$k_1 = k_2(\sqrt{1+\eta^2}-\eta)$
Dimensionless sediment conductance parameter σ: if $\sigma < 0.073$ there is full cutoff; if $\sigma > 19.5$ the sediment is fully pervious. Values described here are at a 5% detection level	$\sigma = p\frac{k_s}{\delta_s}\sqrt{\frac{2}{fs_cT}}$
Dimensionless stream-aquifer interaction parameter χ: with no sediments, if $\chi > 27.5$, there is cutoff and therefore no interaction. If $\chi < 0.1$, there is full interaction and the canal and the aquifer move in unison. Values described here are at a 5% detection level.	$\chi = B\sqrt{\frac{f}{Ts_c}}$
Stream-aquifer interaction parameter modified by sediment resistance; if $\chi > 27.5$ there is cutoff or no interaction; if $\chi' < 0.1$, there is full interaction.	$\chi' = \frac{\chi}{\alpha_s(\sigma)n(\eta)}$
Water level response per for a given discharge impulse $\xi(\chi',\sigma)$ with $0 < \xi < 1.0$. If $\xi > 0.95$, there is no interaction; if $\xi < 0.05$ there is full cutoff at a 5% detection level.	$\xi = \frac{H_0 fB}{q_0}$
Phase lag between discharge impulse and head response, $\theta(\chi',\sigma)$ with $0 < \theta < \pi/4$. With no interaction, $\theta = 0$.	θ

Table 2: Amplitudes and phases of observed data fitted to $Y = a\ \sin(ft + b)$

Gage		Least square method			Cross correlation method			Manual method	
Name	Dist.	a	b	s_e	H/H_c	b	$corr$	a	b
	m	m	rad	m		rad		m	
L-31W	0	0.193	0.000	0.027	1.000	-	-	0.183	0.000
NTS6	14	0.126	0.065	0.029				0.123	0.065
NTS5	17	0.124	0.065	0.031				0.120	0.065
NTS4	21	0.115	0.098	0.031				0.108	0.098
NTS1	280	0.112	0.317	0.017	0.533	0.267	0.98	0.109	0.263
NTS10	1510	0.072	0.396	0.022	0.317	0.377	0.90	0.076	0.458
NTS18	235	0.117	0.327	0.018	0.568	0.052	0.99	0.111	-
NTS1.16	238	0.102	0.258	0.028				0.111	0.208
E112	1490	0.042	1.520	0.014	0.153	-	0.87	0.037	-
FROGP+	1698	0.032	1.741	0.015	-	-	-	0.031	0.625
FROGPD2	2612	0.031	1.770	0.016	-	-	-	0.030	0.624
Q	0	5.805 m^3/s	-0.690	1.796	-	-	-	-	-

$a =$ amplitude of the sine representation $y = a\ \sin(ft + b)$

$b =$ phase of the sine representation

$corr =$ correlation coefficient between gage and canal water levels

$s_e =$ standard error estimate

Table 3: Table of the slopes and the intercepts the fits of log amplitude and phase

Method	Linear plot of log ampl		Linear plot of phase lag	
	intercept $(-\ln(\alpha_s))$	slope (k_1)	intercept (φ_s)	slope (k_2)
Least square, (overall)	4.638×10^{-1}	3.467×10^{-4}	1.550×10^{-1}	1.905×10^{-4}
Cross Corr. (overall)	4.826×10^{-1}	4.438×10^{-4}	1.116×10^{-1}	1.787×10^{-4}
Manual (overall)	4.304×10^{-1}	2.985×10^{-4}	1.058×10^{-1}	2.491×10^{-4}
Least square, (NTS1,NTS10)	4.259×10^{-1}	3.699×10^{-4}	3.078×10^{-1}	5.894×10^{-5}

Table 4: Table of dimensionless parameters

Domain	Overall	Overall	Overall	Zone NTS1,NTS10
Method	LSQ	Cross corr	Manual	LSQ
η	0.635	1.040	0.182	3.058
k_0	2.473×10^{-4}	2.831×10^{-4}	2.636×10^{-4}	1.866×10^{-4}
σ (ampl)	2.503	2.604	2.339	3.749
σ (phase)	3.527	4.065	7.764	-
α_s (ampl)	0.629	0.617	0.650	0.653
ξ (ampl)	0.254	0.254	0.254	0.254
χ (ampl)	0.405	0.412	0.397	0.501
χ (phase)	0.688	0.844	0.452	1.332
θ	0.690	0.690	0.690	0.690

Explanations

(ampl) = Values computed using ξ or amplitude ratio of head and discharge

(phase) = Values computed using θ or the phase lag between head and discharge

Table 5: Table of primitive variable computed using various methods

Domain	Overall	Overall	Overall	Zone NTS1, NTS10
Method	LSQ	Cross corr	Manual	LSQ
1. Aquifer diffusivity T/s_c, (m^2/s)	297	227	261	522
2. Ampl based diffusivity T/s_c, (m^2/s) (assuming non-leaky)	151	92	204	132
3. Aquifer T s_c (ampl), (m^2/s)	0.0742	0.0716	0.0768	0.0484
4. Aquifer T s_c (phas), (m^2/s)	0.0257	0.0170	0.0595	0.0068
5. Transmissivity T,(ampl) m^2/s	4.69	4.03	4.48	5.03
6. Transmissivity T,(phas) m^2/s	2.76	1.96	3.94	1.89
7. Storage coeff s_c	0.0158	0.0177	0.0171	0.0096
8. Coeff of leakage (sediment) k_s/δ_s (day^{-1})	13.72	14.03	13.06	16.62
9. Coeff of leakage (aquifer) k_v/δ_v (day^{-1})	0.0315	0.0581	0.0098	0.0925

Explanation of the rows in the table

2. Referred to as effi ciency based diffusivity by Carr and Van Der Camp (1969)

3. Computed using ξ or amplitude ratio of head and discharge

4. Computed using θ or the phase lag between head and discharge

5. Computed using ξ or amplitude ratio of head and discharge

6. Computed using θ or the phase lag between head and discharge

FIGURES

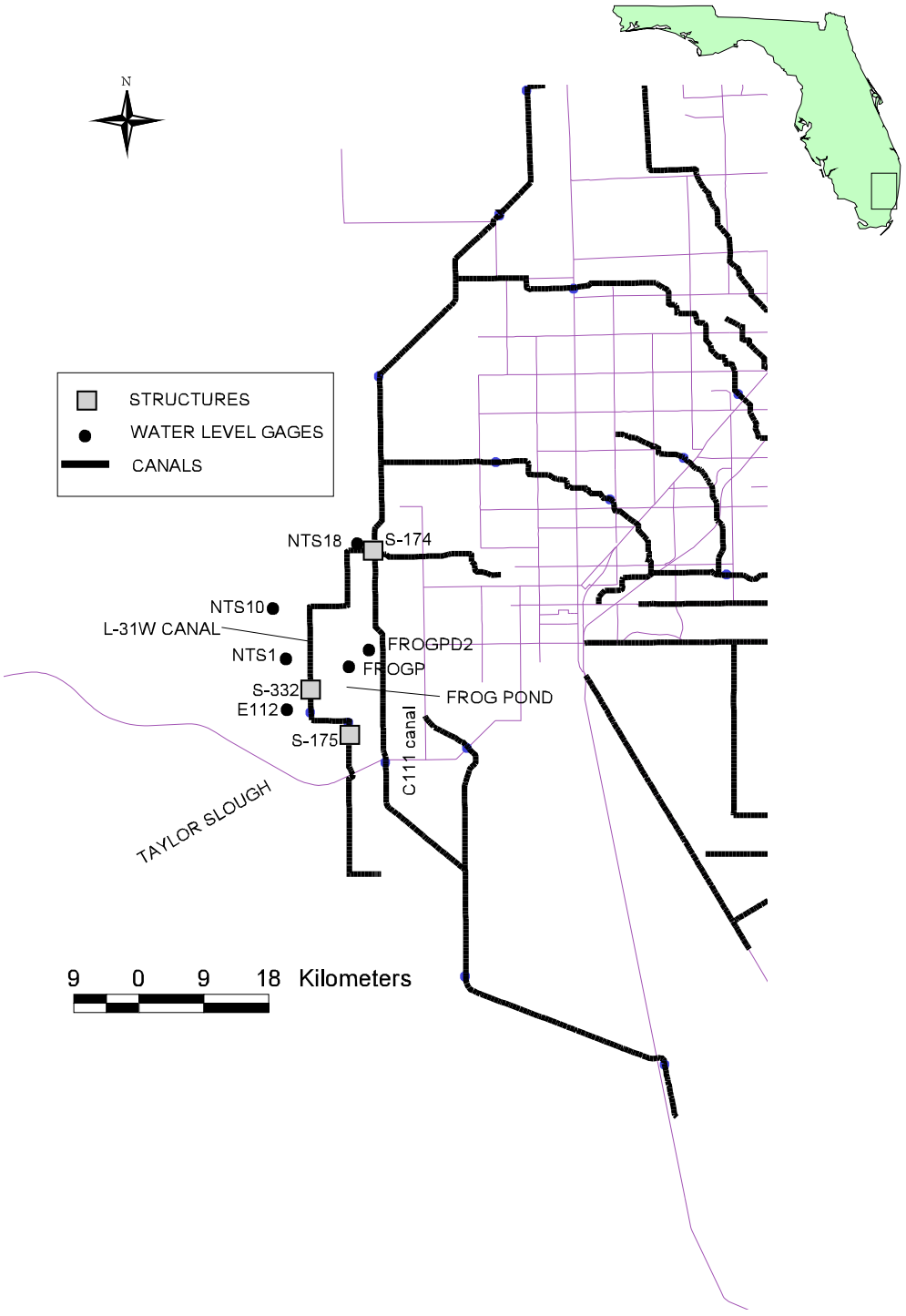

Figure 1: Study site in Dade County, Florid showing the canals and the structures

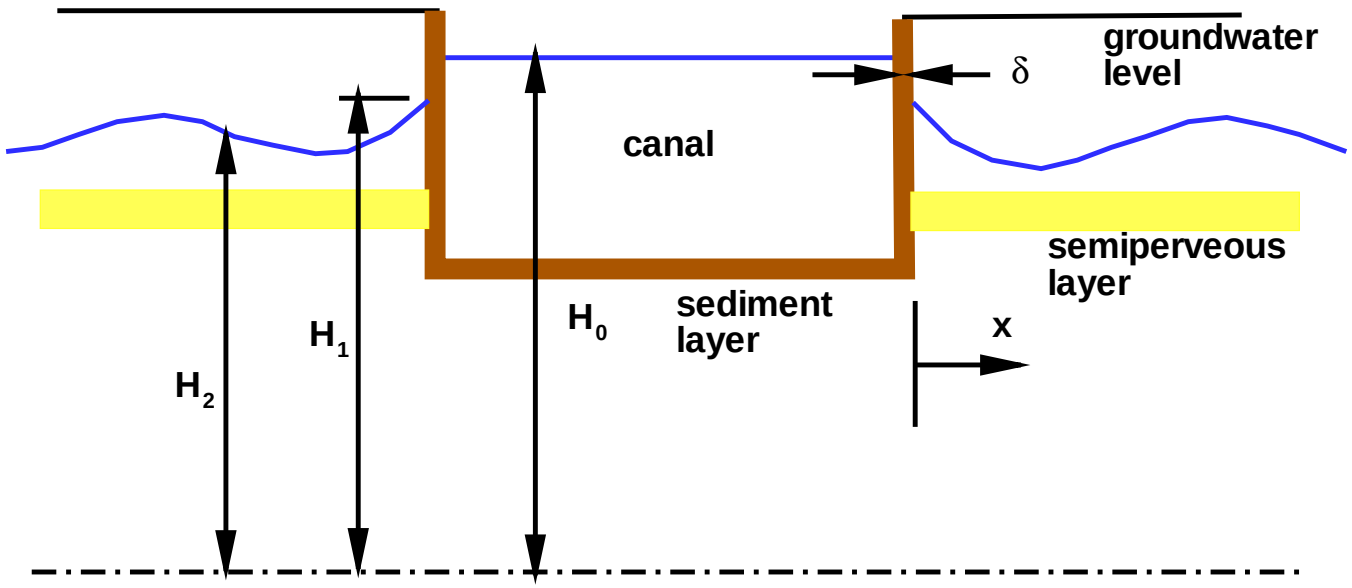

Figure 2: Definition sketch of a canal cross section

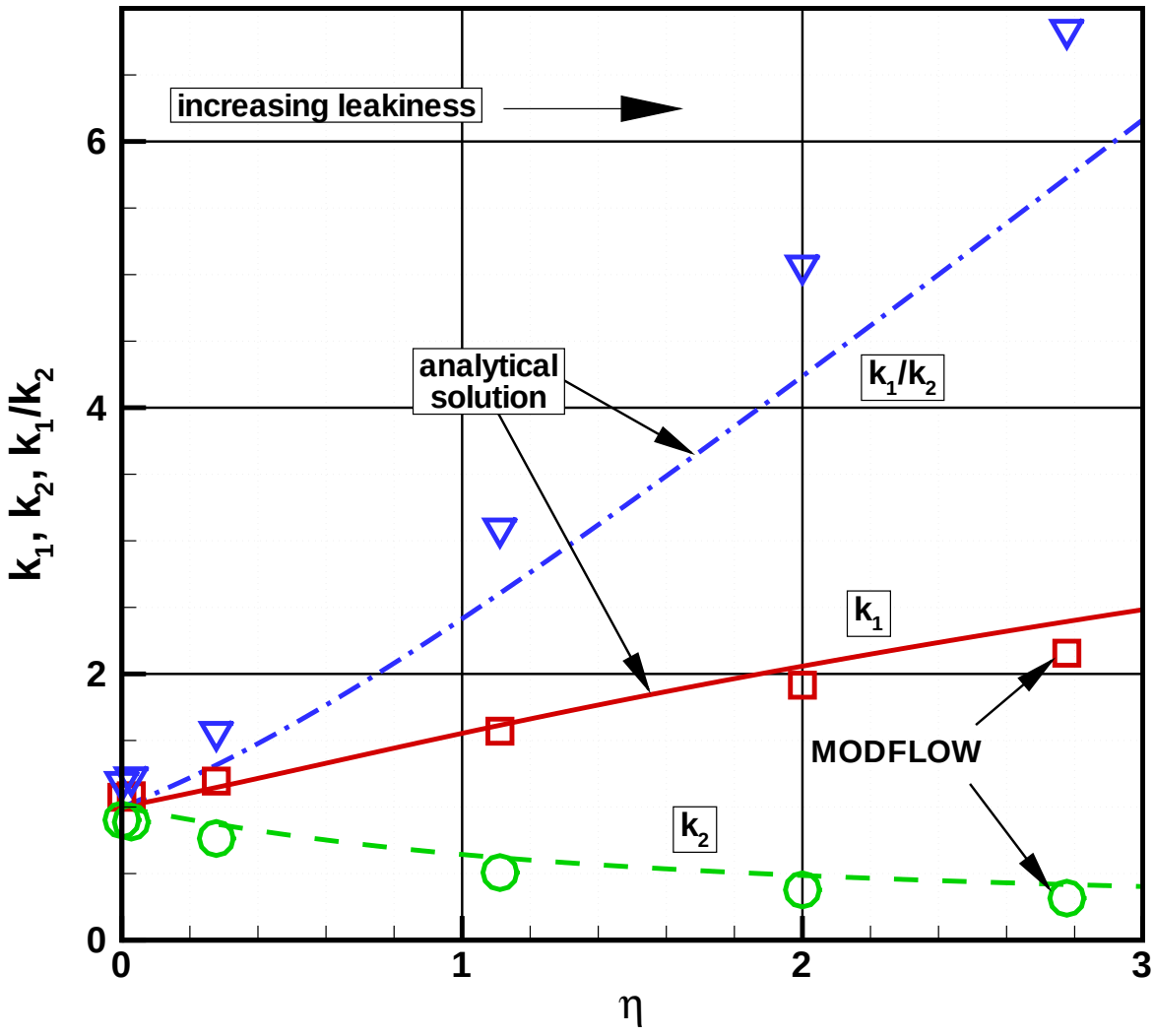

Figure 3: Plot of decay constant k_1, delay constants k_2, and k_1/k_2 with vertical leakiness parameter η

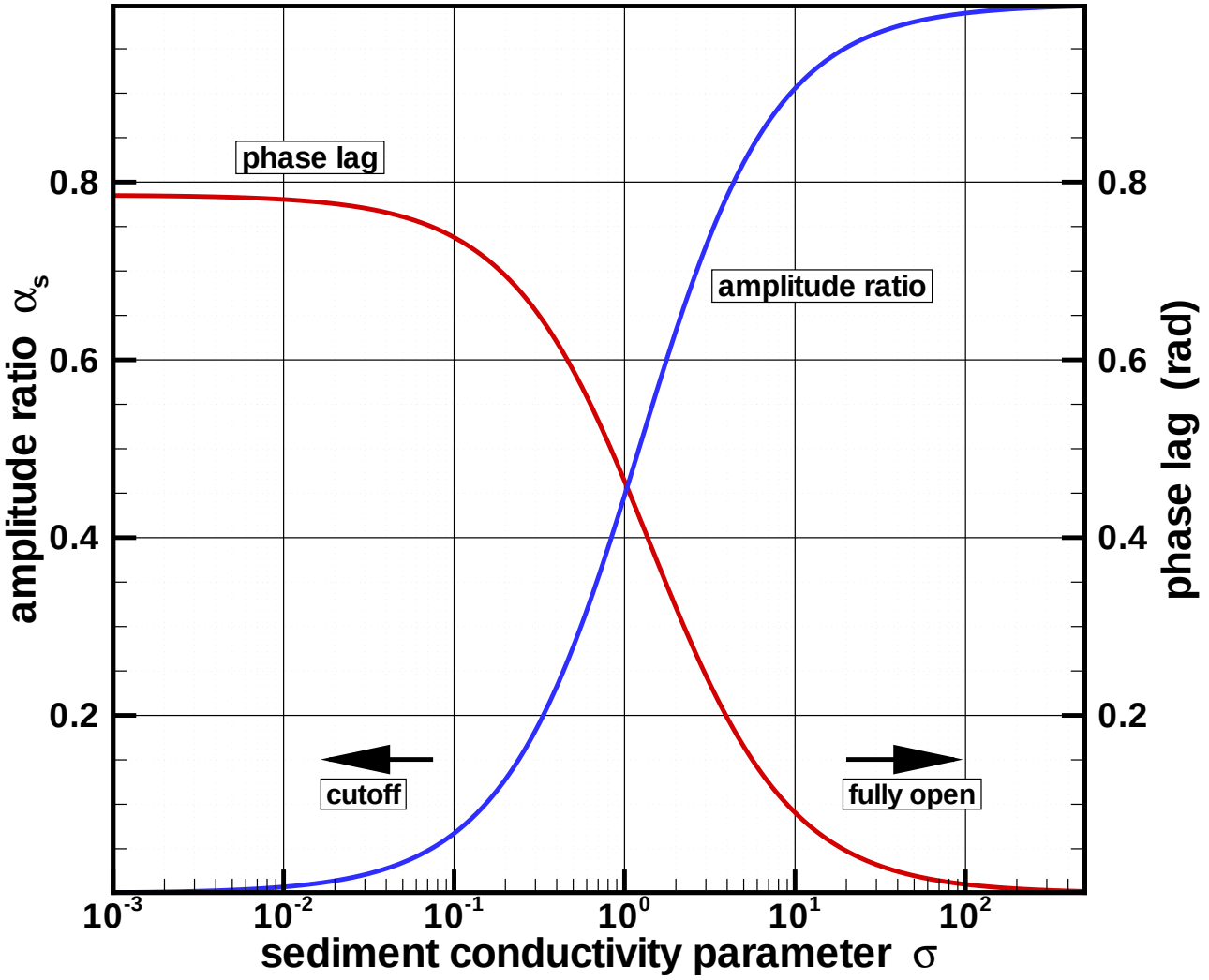

Figure 4: Plot of amplitude attenuation α_s and phase lag φ_s across the sediment layer versus σ. This plot is similar to a plot of ξ and θ versus $\chi'/\sqrt{2}$

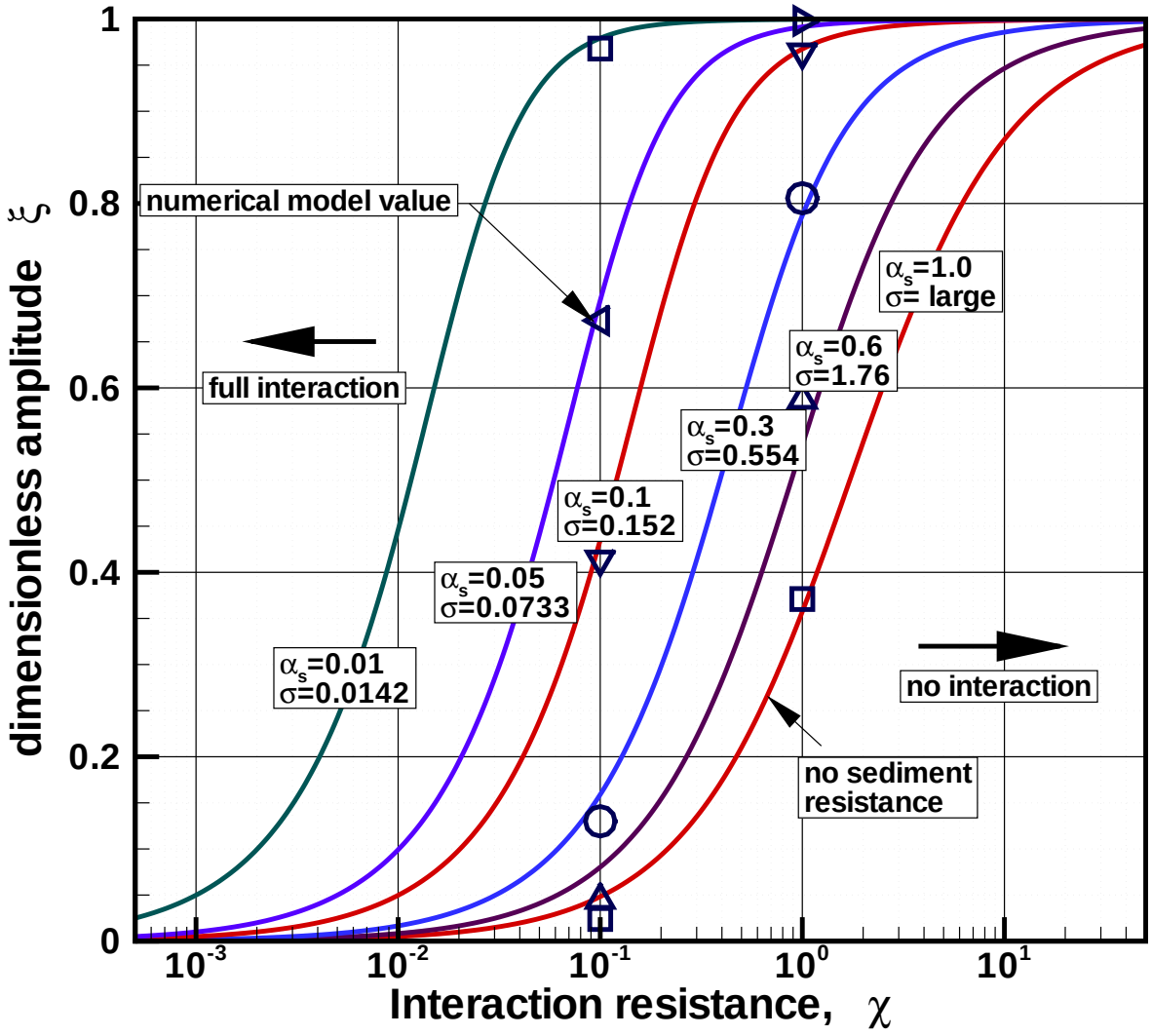

Figure 5: Plot of ξ versus χ and σ

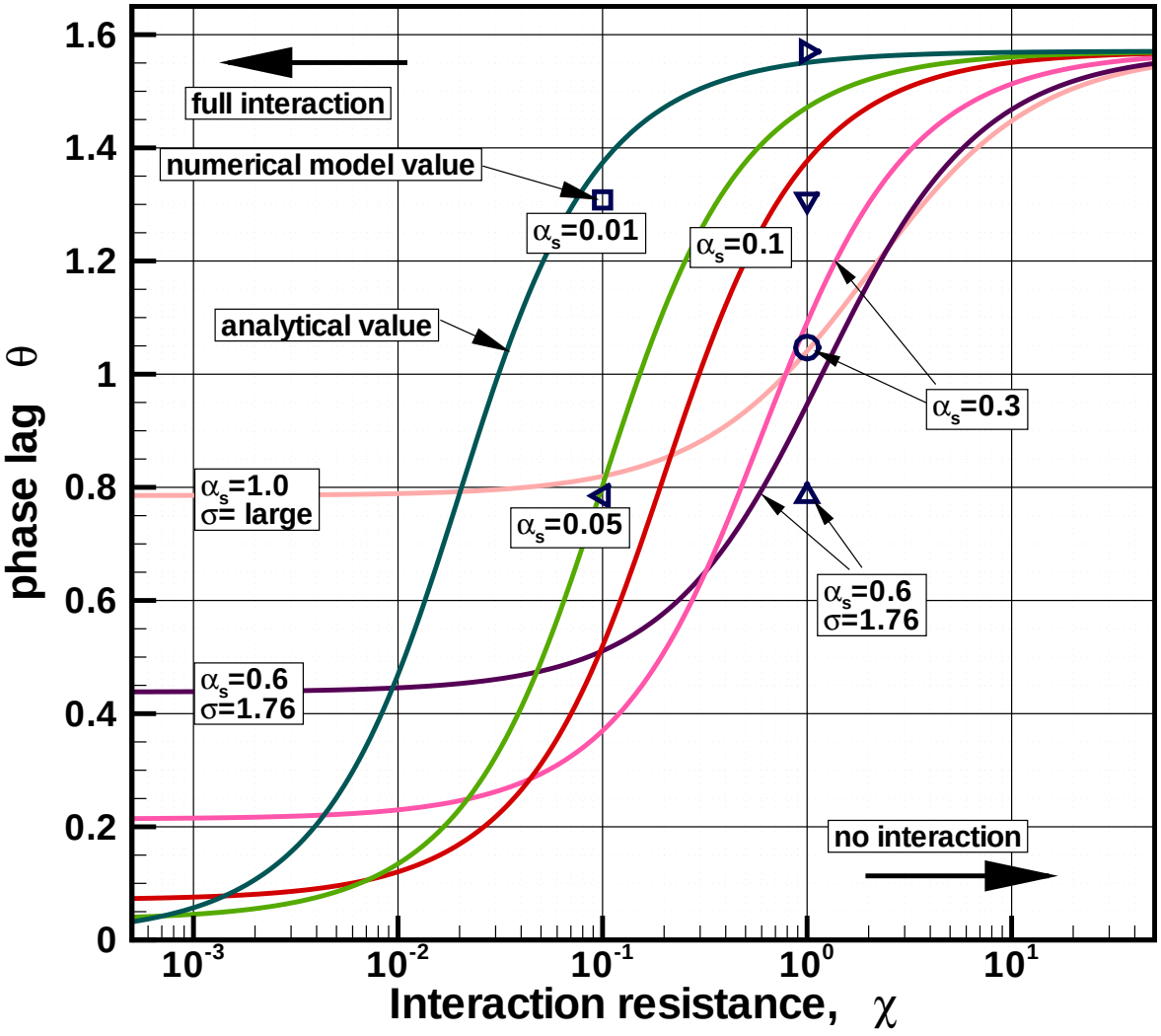

Figure 6: Plot of θ versus χ and σ

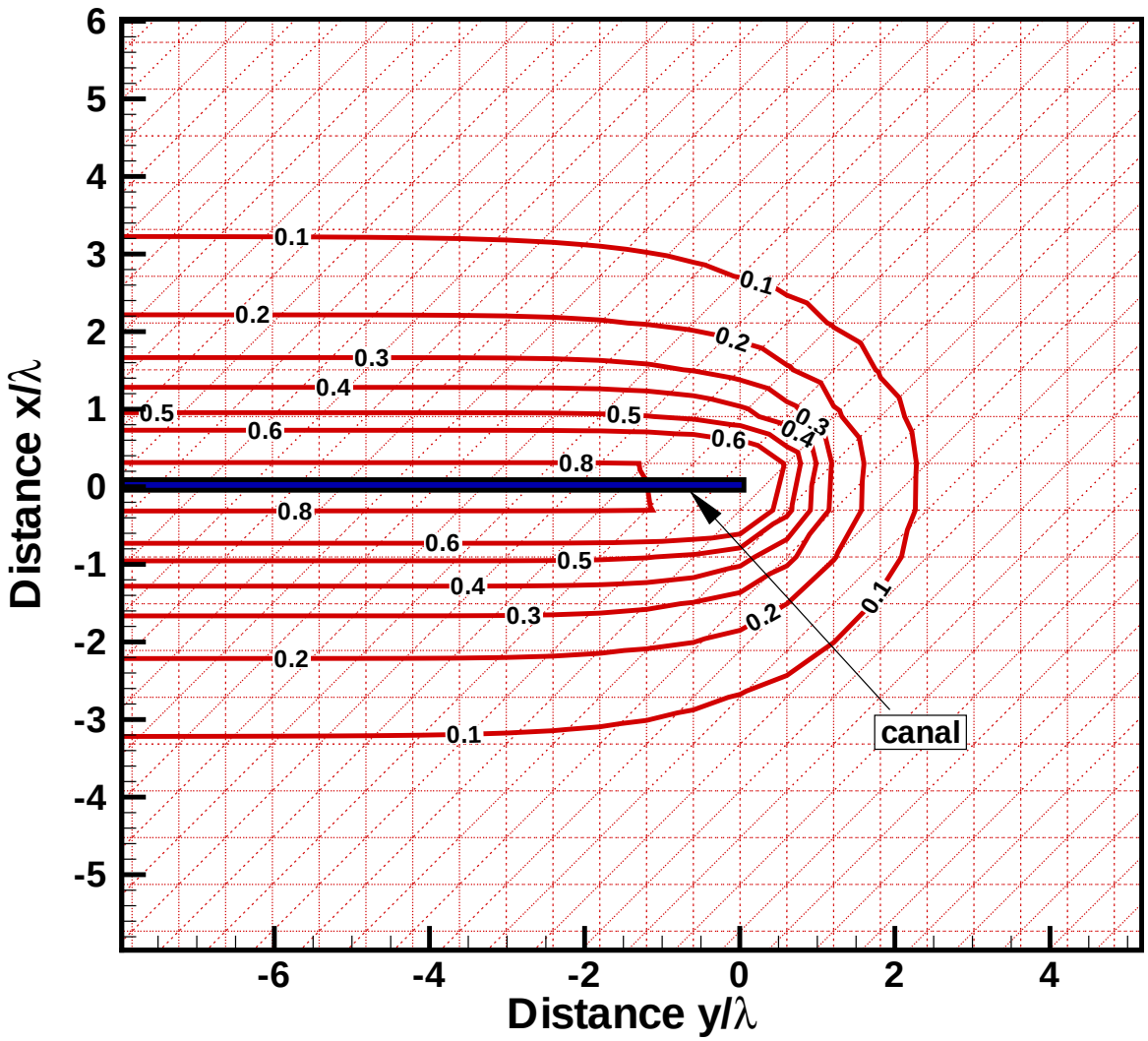

Figure 7: Contours of dimensionless amplitudes H/H_0 at a canal end obtained using RSM. H_0 is the maximum analytical water level at the canal

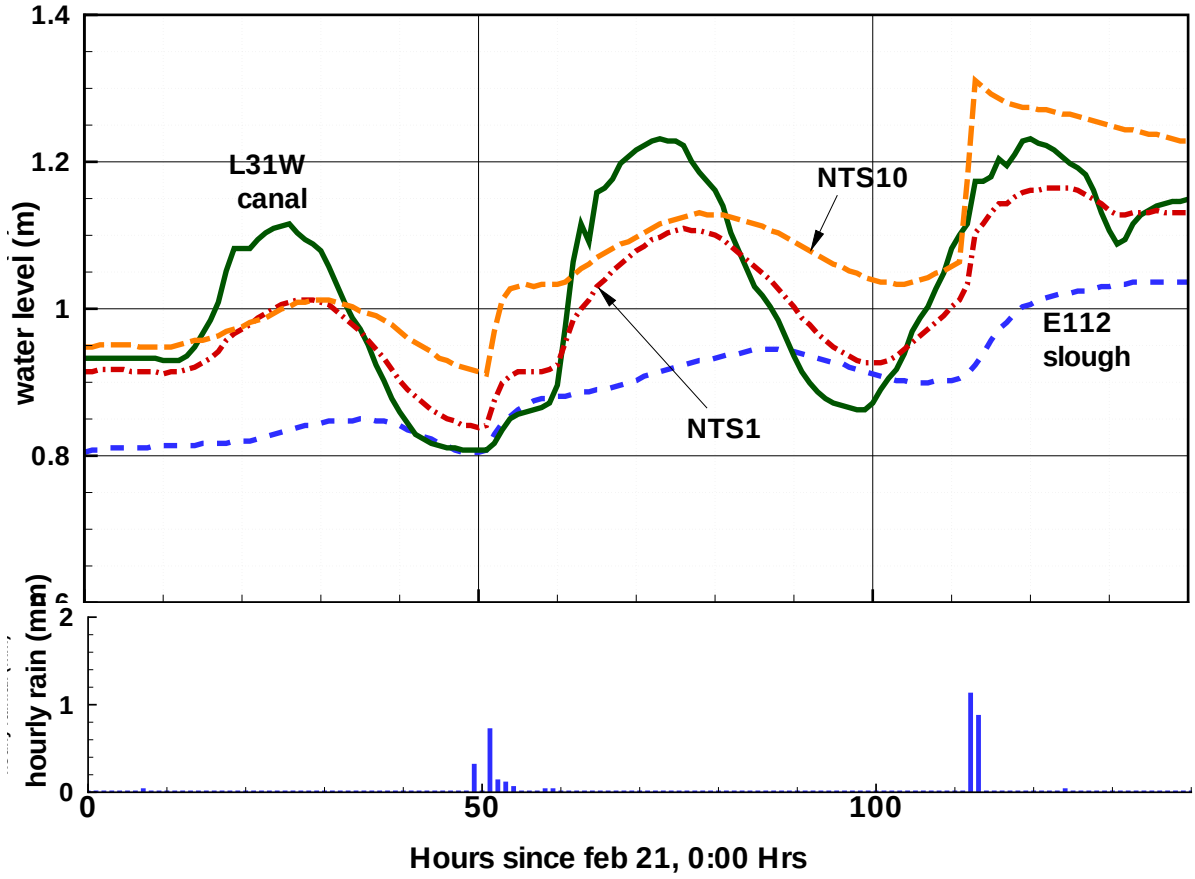

Figure 8: Raw time series data and rainfall for selected stations.

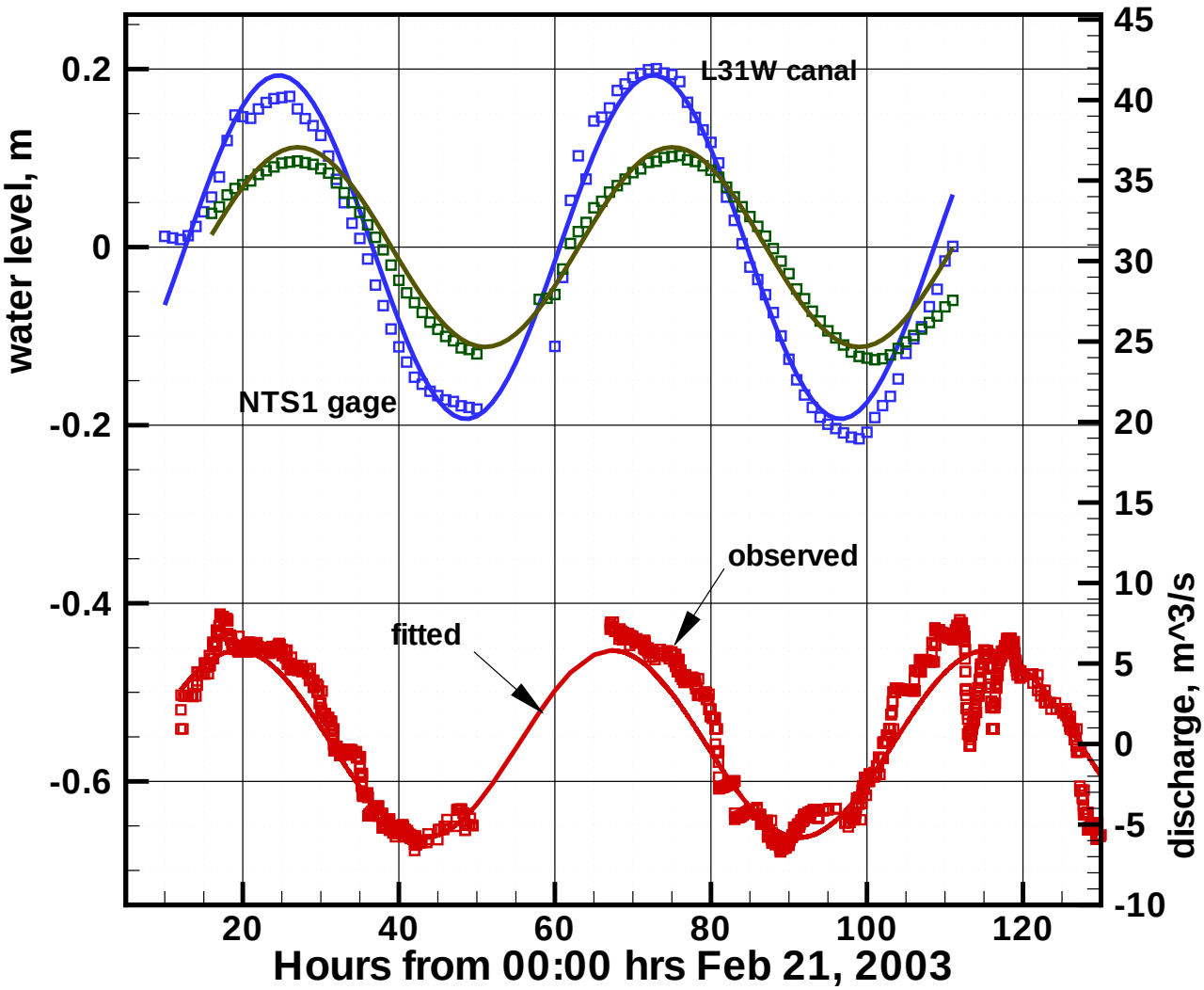

Figure 9: Water level and net inflow rate data and their sinusoidal fits

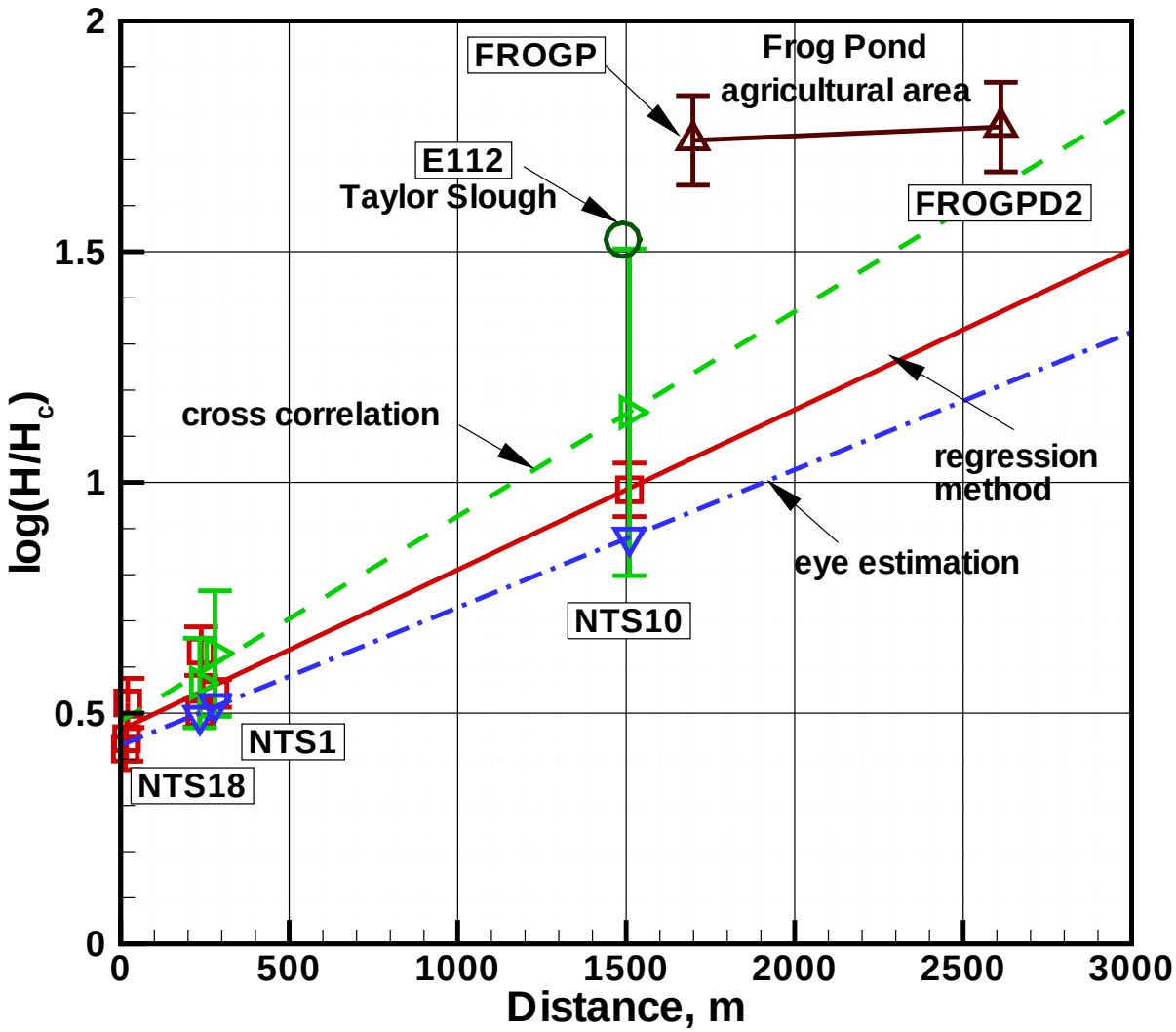

Figure 10: Plot of $\log(H/H_0)$ against distance from gage to canal

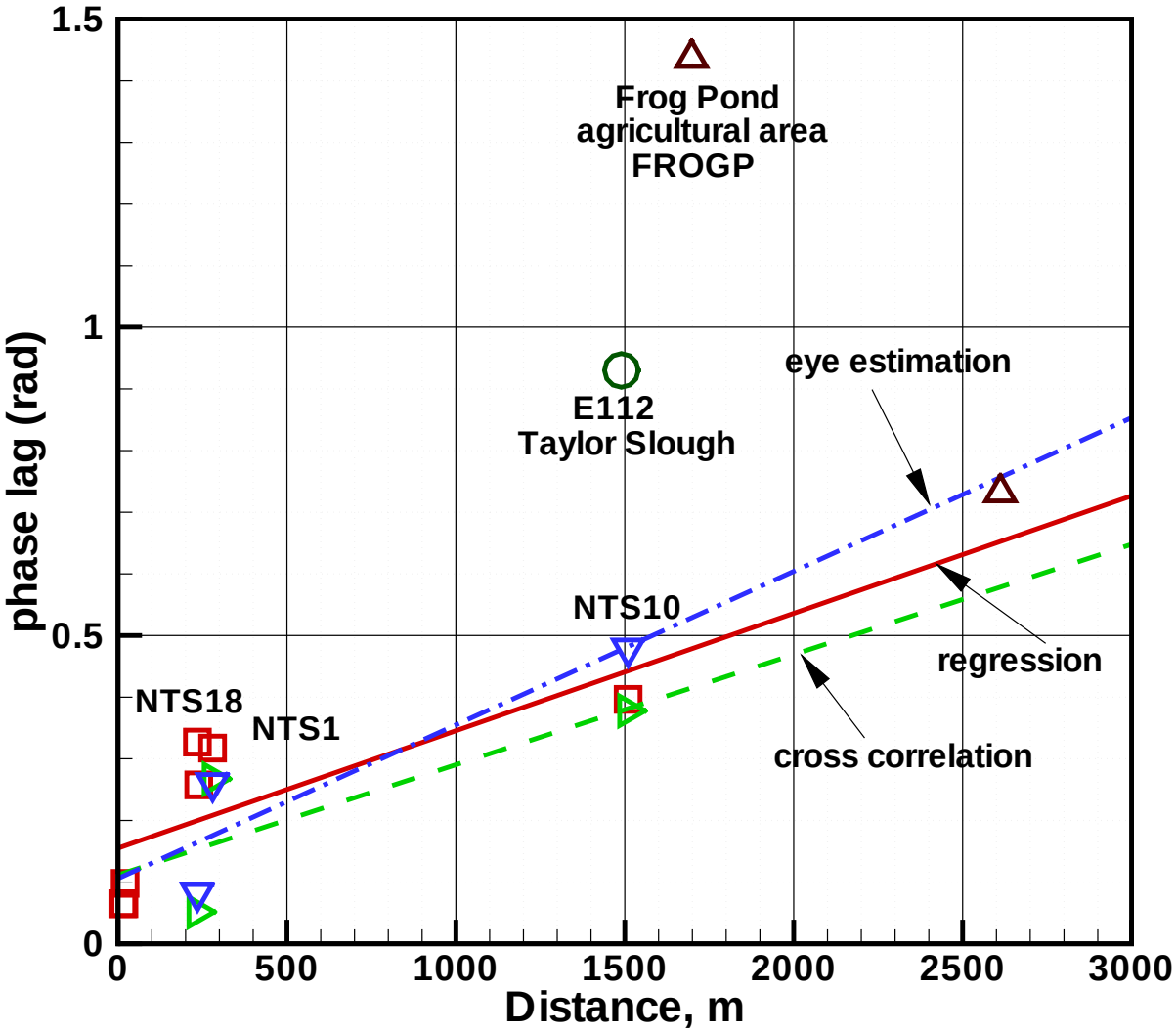

Figure 11: Plot of phase lag versus the distance from gage to canal